RSC Advances

PAPER

View Article Online
View Journal | View Issue

Cite this: *RSC Adv.*, 2025, **15**, 27782

Synthesis and catalytic application of bimetallic-MOFs in synthesis of new class of phenylnicotinonitriles

Mahrokh Farrokh,[a] Mohammad Ali Zolfigol,*[a] Maryam Hajjami,*[a] Hassan Sepehrmansourie*[b] and Milad Mohammadi Rasooll[a]

Today, the development of porous catalysts for catalytic purposes is being targeted. Herein, this goal was pursued by using the porous substrate of the metal–organic frameworks (MOFs). First, MIL-88B(Fe_2/Co)-TPA-$Cu(OAc)_2$ as a new catalyst containing copper complex based on Fe and Co-based bimetallic-MOFs was synthesized by using back-to-back solvothermal and reflux methods. The structure of the catalyst was investigated and proved using different methods such as FT-IR, XRD, SEM, EDX, Elemental mapping, XPS, BET/BJH and TGA/DTG. The catalytic activity of the target structure was studied in the preparation of new phenylnicotinonitriles. The results of various investigations showed that MIL-88B(Fe_2/Co)-TPA-$Cu(OAc)_2$ has good activity in the synthesis of phenylnicotinonitriles and performs these reactions in green and mild conditions. The last step of synthesis has proceeded *via* a cooperative vinylogous anomeric based oxidation. The structure of the synthesized compounds was identified and confirmed using melting point, FT-IR, ^{1}H-NMR and ^{13}C-NMR techniques. The recyclability of the catalyst was also investigated and good results were obtained. The mentioned properties of this prepared catalyst make it a suitable porous catalyst.

Received 9th June 2025
Accepted 18th July 2025

DOI: 10.1039/d5ra04067a

rsc.li/rsc-advances

1. Introduction

The modification of heterogeneous catalysts with metals has become important in many chemical reactions. Meanwhile, Cu metal has been used more because it is easier to access economically and environmentally. Also, Cu metal has shown a good catalytic application for various purposes. Copper complex is widely used as a catalyst in many organic reactions such as oxidation, Sonogashira coupling and catalytic organic reactions.[1,2] Porous organic polymers (POPs), covalent organic frameworks (COFs) and metal–organic frameworks (MOFs) are three groups of heterogeneous catalysts that are used as substrates for the post-modification.[3] In recent years, our research group has been introduced various functionalized catalysts using the post-modification method on carbon quantum dots (CQDs),[4] mesopores silica,[5,6] MOFs[7–10] and organic materials such as uric acid,[11] melamine[12] and glycoluril.[13–15] Recently we have comprehensively reviewed a new perspective on the design and synthesis of the heterocyclic-linked COFs.[16] To the best of our knowledge, the catalytic application of metal–organic frameworks, especially bimetallic-MOFs, has been identified as an important group of porous compounds. In recent years, with the advancement of science and technology, the design of efficient nanoreactors with unique properties has been received more attention. Porous materials have become very important because they are the basis of many researches.[17,18] Metal–organic frameworks (MOFs) as a distinctive category of porous materials are a type of extended crystalline materials made by bonding metals with organic ligands. This category of porous materials is very important because it is adjustable and by changing the designed ligands or using different metals, many MOFs can be synthesized.[19,20] In addition, the functionalization of MOFs can occur *via* post-modification methodologies. Very recently, the disciplines of designing and processing MOFs for specific applications have been comprehensively reviewed.[21] Compared to other porous materials that exist in different forms, MOFs have unique properties such as higher surface area, larger pores, and fine-tuning of the structure at the molecular level.[22] This type of diversity has caused these porous compounds to be used in various fields such as heterogeneous catalysts, photocatalysts, adsorption and absorption, gas storage, optoelectronic materials, separation, molecular sensing and identification, drug delivery, *etc.*[23–25] One of the most important uses of MOFs is their catalytic utilities and/or applications.[26] In recent years, the design of MOF using mixed metals has also attracted a lot of attention.[27] In this type of structure, due to the

[a]*Department of Organic Chemistry, Faculty of Chemistry and Petroleum Sciences, Bu-Ali Sina University, Hamedan 6517838683, Iran. E-mail: zolfi@basu.ac.ir; mzolfigol@yahoo.com; m.hajjami@basu.ac.ir; mhajjami@yahoo.com; Fax: +988138380709; Tel: +988138282807*

[b]*Faculty of Converging Science and Technologies, University of Qom, Qom, 37185-359, Iran. E-mail: Sepehr9129@yahoo.com*

presence of more than one metal, the creation of defects and synergistic effect between two metals in bimetallic-MOFs can lead to increased their catalytic activity.[28] The choice of metals in these structures is very important because they must be harmonious. In this context, Fe and Co metals had been shown their importance and characteristics.[29] The simultaneous presence of these two metals in their structure increases the stability of the bimetallic-MOFs and affects their morphology.[30] Heterocycles are an important group of organic compounds that form the basis of many biologically active molecules, pharmaceutical, health and environmental compounds.[31] Phthalimide, indole, pyridine and nicotinonitriles are among the most prominent heterocyclic nuclei that have various properties such as anti-tumor, anti-viral, anti-inflammatory, and antifungal properties that have the ability to expand widely and have various applications in the fields of medicine, cosmetics health and agriculture. Materials with these cores are used in many products such as adhesives, food flavors, pharmaceuticals, dyes, insecticides, vitamins, and herbicides.[32–34] Fig. 1 shows a number of medicinal substances with pyridine, indole, phthalimide and nicotinonitriles building blocks, whose properties have been proven.[35–39] Anomeric effect (AE) as a fundamental subset of stereoelectronic interactions has a great educational and research applications.[40–43] This concept had been introduced in 1955 by J. T. Edward in his studies on the carbohydrate chemistry.[44] The reported theory for the development of anomeric effect (AE) concept had been proposed that sharing the lone pair's electrons of heteroatoms (X: N, O) to the anti-bonding orbital C–Y ($n_X \rightarrow \sigma^*_{C-Y}$) and weakened it (Fig. 2). Stereoelectronic effects have also a major role in the oxidation–reduction of susceptible biological compounds such as NADPH/NADP$^+$ (Fig. 3).[45] Recently, we and our coworkers have reviewed the role of the above-mentioned fundamental concepts comprehensively.[46–48]

Since that modifying the bimetallic-MOFs with Cu metal can be an attractive idea that has been addressed in this research. In continuation of our previous research in the design of targeted catalysts,[8,49,50] in this research, the aim is to design a new bimetallic-MOFs based on Fe and Co, which are in good compatibility with each other. Next, the main goal is to put Cu on it to create a copper complex on bimetallic-MOFs to convert this structure into a suitable heterogeneous porous catalyst. Catalyst MIL-88B(Fe_2/Co)-TPA-Cu(OAc) as an efficient porous catalyst will be used in the synthesis of a new class of phenylnicotinonitriles to determine its catalytic ability. Synthesized phenylnicotinonitriles can be suitable candidates for medical and environmental uses due to the presence of biological nuclei such as pyridine, indole, phthalimide and nicotinonitriles (Fig. 4).

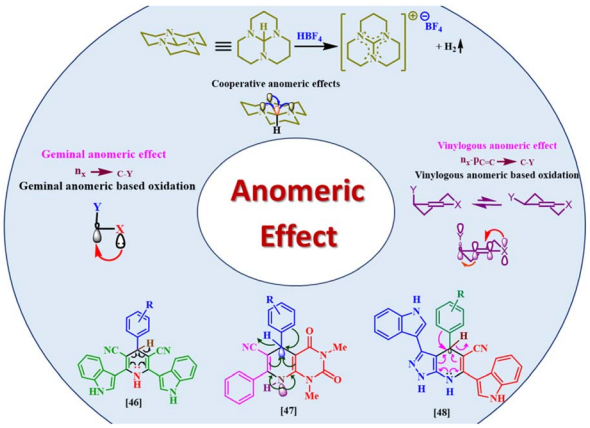

Fig. 2 The geminal *versus* vinylogous anomeric effect in organic synthesis.

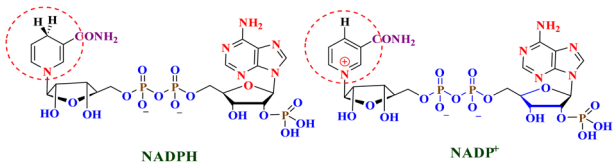

Fig. 3 The structures of NADPH/NADP$^+$.

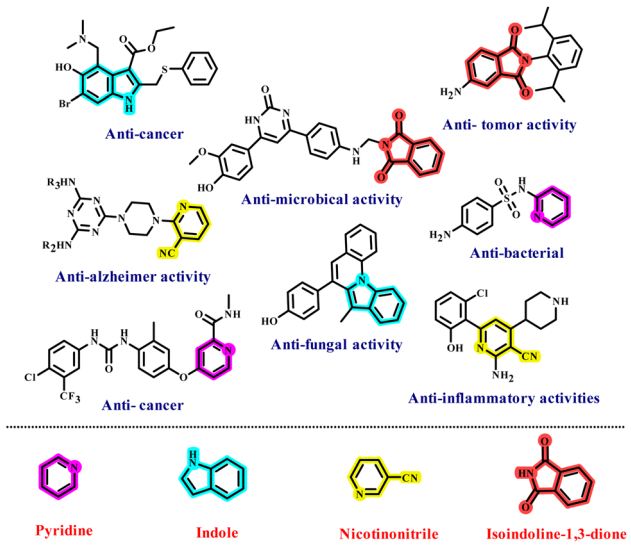

Fig. 1 Some structure of medicinal compounds containing pyridine, indole, phthalimide and nicotinonitriles moieties.

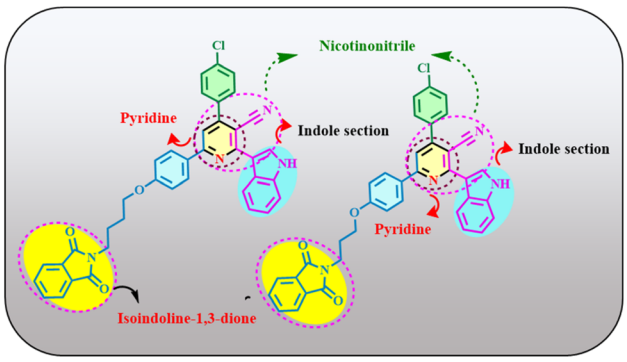

Fig. 4 Target synthesized molecules with pyridine, indole, phthalimide and nicotinonitriles moieties.

2. Experimental section

2.1 Materials and methods

All materials and solvents used in this work such as $FeCl_3 \cdot 6H_2O$ (Merck, 99%), $Co(NO_3)_3 \cdot 6H_2O$ (Merck, 99%), 2-amino terephthalic acid (NH_2-BDC, Merck, 95%), *tert*-butyl nitrite ($(CH_3)_3$-CONO, Merck, 95%), trimethylsilyl azide (TMS-N_3, Merck, 95%), 4-hydroxy acetophenone (Merck, 99%), potassium carbonate (Merck, 99/5%), propargyl bromide (Merck, 80%), indole (Merck, 99%), phthalimide (Merck, 99%), aldehyde derivatives, acetic anhydride (Merck, 98.5%), 1,3-dibromopropane (Merck, 99%), 1,4-dibromobutane (Merck, 98.5%), ammonium acetate (Merck, 99%), 2-aminopyridine (Merck, 99%), EtOH (Merck, 99%), copper(II) acetate (Merck, 98%), cyanoacetic acid (Merck, 98%), dry-tetrahydrofuran (Merck, 99.5%) and *N*,*N*-dimethylformamide (DMF, Merck, 99%) were obtained from commercial sources without further purification. The required raw materials were synthesized according to our recently reported educational synthetic methodology.[51]

2.2 Instrumentation

The X-ray Powder Diffraction (XRD) technique with a model device PHILIPS PW1730 (Netherlands), was used to characterize the crystal plates of the presented catalyst. The FT-IR technique model device (PerkinElmer Spectrum Version 10.02.00) was used to identify the functional groups of the different stages of the catalyst. Moreover, the morphology of the different stages of catalyst was characterized using a scanning electron microscope (SEM) technique as well as energy-dispersive spectroscopy (EDS) and elemental mapping was carried out by the model ZEISS Sigma VP (German) and SEM quanta 200-EDAX silicon drift 2017. Analysis XPS was performed with BESTEC model EA 10 (German) device. In addition, the thermal and chemical stability of the catalyst was determined using a thermogravimetry/differential thermal analysis (TGA/DTA) technique (BAHR STA 503). Finally, the Brunauer–Emmett–Teller (BET, BELSORP-mini-II) Barrett–Joyner–Halenda (BJH) technique with a model device BELSORP-mini-II was utilized to determine the surface area and pore size of the synthesized catalyst.

2.3 Preparation of MIL-88B(Fe_2/Co)-NH_2

MIL-88B(Fe_2/Co)-NH_2 as bimetallic-MOFs was synthesized according to the previously reported method.[50,52] First, BDC-NH_2 (2 mmol, 0.362 g) was dissolved in 7.5 mL of DMF. Simultaneously, $FeCl_3 \cdot 6H_2O$ (1.33 mmol, 0.359 g) and $Co(NO_3)_3 \cdot 6H_2O$ (0.66 mmol, 0.192 g) were dissolved in 7.5 mL of DMF. The final mixture obtained by mixing two solutions was stirred for 60 minutes at 25 °C. Then the contents were transferred to a 60 mL autoclave and placed at 120 °C. After 24 h, the precipitate was washed several times with DMF and EtOH and then dried at 100 °C for 12 h (Scheme 1).

2.4 Preparation of MIL-88B(Fe_2/Co)-N_3

To perform the next step, 0.1 g of bimetallic-MOFs was placed into a 10 mL round bottom flask in 2 mL of THF at 0–5 °C. *Tert*-butyl nitrite (0.570 mL, 4.82 mmol) was added to it. After 15 min, trimethylsilyl azide (0.439 mL, 3.82 mmol) was added dropwise to the contents of the flask. The obtained reaction mixture was stirred at 0–5 °C for 20 minutes. Then the reaction mixture was stirred at 25 °C for 6 h. After completion of the reaction, the reaction mixture was washed several times with THF. The obtained MIL-88B(Fe_2/Co)-N_3 was dried at 80 °C (Scheme 1).

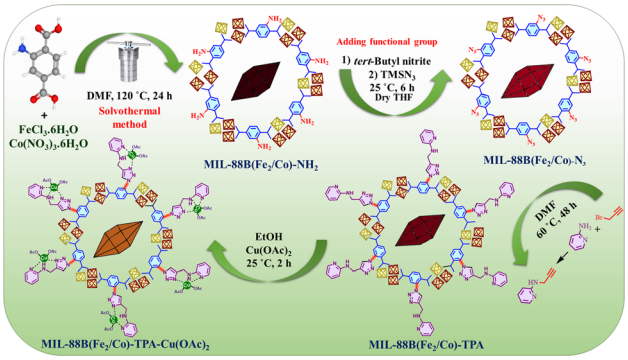

Scheme 1 Preparation of MIL-88B(Fe_2/Co)-TPA-Cu$(OAc)_2$ as an efficient porous catalyst containing copper complex based on Fe and Co-based bimetallic-MOFs.

2.5 Preparation of MIL-88B(Fe_2/Co)-TPA-Cu$(OAc)_2$ as an efficient porous catalyst

To perform the next step, using 2-aminopyridine and propargyl bromide, the precursor of the ligand was synthesized according to the previously reported method.[53] After, 0.1 g MIL-88B(Fe_2/Co)-N_3 was poured into 2 mL of DMF solvent in a 10 mL round-bottom flask, and 0.1 g of *N*-ethynylpyridin-2-amine, 0.2 mL of triethylamine, and of CuI (0.1 g) were added to it. The resulting mixture was stirred at 60 °C for 48 h. After the reaction was completed, the reaction mixture was washed several times with DMF. The obtained MIL-88B(Fe_2/Co)-TPA (TPA: triazole pyridine amine) was dried at 80 °C. In the following, a mixture of MIL-88B(Fe_2/Co)-TPA (0.5 g) and $Cu(OAc)_2$ (0.1 mmol, 0.018 g) were stirred in EtOH (20 mL) as a solvent in 25 °C for 2 h. Then, MIL-88B(Fe_2/Co)-TPA-Cu$(OAc)_2$ was dried at 60 °C to create a copper complex based on bimetallic-MOFs as a desired porous catalyst (Scheme 1).

2.6 Catalytic reaction

2.6.1 Synthesis of raw materials. The synthesis of raw materials was carried out according to the following method: first, in a 50 mL round bottom flask, phthalamide (10 mmol, 1.47 g) with 3-carbon or 4-carbon dibromo compounds (23 mmol) and K_2CO_3 (15 mmol, 2.07 g) were mixed in 20 mL of DMF as a solvent for 24 h at room temperature. After the reaction was completed, the reaction mixture was decanted with EtOAc and H_2O solvents. The organic layer was separated and dried by adding anhydrous sodium sulfate. After drying the solution its organic solvent was evaporated. The compound A was obtained. Next, in a 25 mL round bottom flask, 4-

hydroxyacetophenone (2 mmol, 0.27 g) with compounds A (3 mmol) and K_2CO_3 (4 mmol, 0.55 g) in 10 mL of DMF as a solvent was stirred at room temperature for 24 h. After the reaction was completed, the reaction mixture was decanted with EtOAc and H_2O solvents. The organic layer was separated and dried by adding anhydrous sodium sulfate. After drying the solution its organic solvent was evaporated. Finaly compounds B and C as raw materials were obtained.[54]

2.6.2 Synthesis of new phenylnicotinonitriles using MIL-88B(Fe_2/Co)-TPA-Cu(OAc)$_2$ as an efficient porous catalyst. The catalytic application of MIL-88B(Fe_2/Co)-TPA-Cu(OAc)$_2$ in the synthesis of a new class of phenylnicotinonitriles was investigated through a multi-component reaction. For this purpose, in a 10 mL round-bottom flask, 1 mmol of compounds B or C as raw materials (0.32 g or 0.334 g), 1 mmol (0.184 g) of 3-(1*H*-indol-3-yl)-3-oxopropanenitrile (synthesized according to the previously reported method[55,56]), ammonium acetate (1.5 mmol, 0.115 g), various aldehyde derivatives (1 mmol), and 20 mg of MIL-88B(Fe_2/Co)-TPA-Cu(OAc)$_2$ as catalyst were stirred under solvent-free conditions at 110 °C. The progress of the reaction was checked out by using the TLC technique. After the completion of the reaction, 5 mL of DMF was added to the reaction mixture for the trituration and isolating of the used catalyst. The catalyst was separated by centrifugation. Next, 5 mL of H_2O was added to the resulting solution and the obtained precipitate was washed using EtOH for purification (Scheme 2). The structures of the synthesized products were evaluated and confirmed by melting point, FT-IR, ^{1}H-NMR and ^{13}C-NMR techniques (see in SI).

3. Results and discussion

Recently, the focus of our research group has been focused on the development of tasked-specific porous catalysts and their functionalization *via* post-modification methodologies.[48–50] Therefore, in this research, we decided to design, synthesize and apply MIL-88B(Fe_2/Co)-TPA-Cu(OAc)$_2$ as a new catalyst containing copper complex based on Fe and Co-based bimetallic-MOFs. The catalytic application of MIL-88B(Fe_2/Co)-TPA-Cu(OAc)$_2$ in the synthesis of a new class of phenylnicotinonitriles containing biological moiety during the multi-component reaction was investigated (Schemes 1 and 2). For the last step of the mechanism in the synthetic methodology a cooperative vinylogous anomeric based oxidation in the formation of pyridine rings was proposed.[57,58]

3.1 Catalyst preparation strategy

In this research, the post-modification method was used to design, synthesize and functionalize the targeted catalyst. For this purpose, bimetallic-MOFs, by using Fe and Co metals were selected and synthesized as a catalytic bed. Next, the NH_2 groups of the synthesized structure were converted to the N_3 group through a diazonium salt intermediate. In the next step, the synthesized compound *N*-ethynylpyridin-2-amine was added to it, so that the structure is ready for the complexation *via* the addition of copper acetate. In the last step, copper acetate was added to create the final porous catalyst containing copper (Scheme 1). The structure of the catalyst and the initial stages of its synthesis have been evaluated using various techniques such as FT-IR, XRD, SEM, EDX, XPS, elemental mapping, BET/BJH and TGA/DTG.

After designing and synthesizing MIL-88B(Fe_2/Co)-TPA-Cu(OAc)$_2$ as an efficient porous catalyst containing copper complex based on Fe and Co-based bimetallic-MOFs, it was used in the synthesis of a new class of phenylnicotinonitriles containing biological section, which are an important category of organic compounds (Scheme 2). Synthesis of products with reasonable yield and short reaction time were the goals achieved by the desired catalyst. The structures of the synthesized products were evaluated and confirmed by melting point, FT-IR,

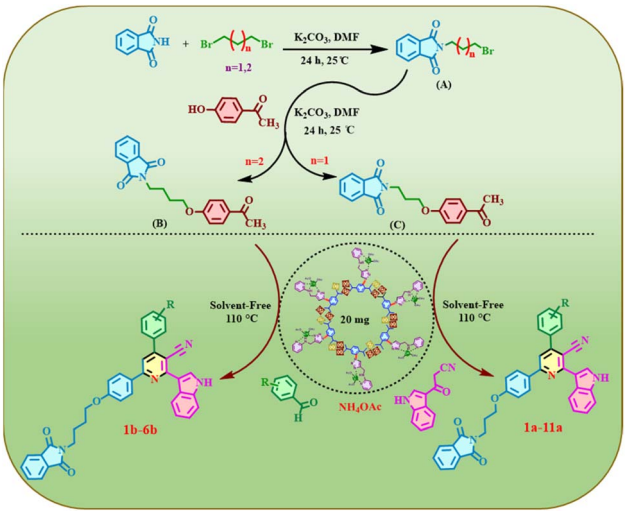

Scheme 2 Preparation of a new class of phenylnicotinonitriles using MIL-88B(Fe_2/Co)-TPA-Cu(OAc)$_2$ as an efficient porous catalyst containing copper complex based on Fe and Co-based bimetallic-MOFs.

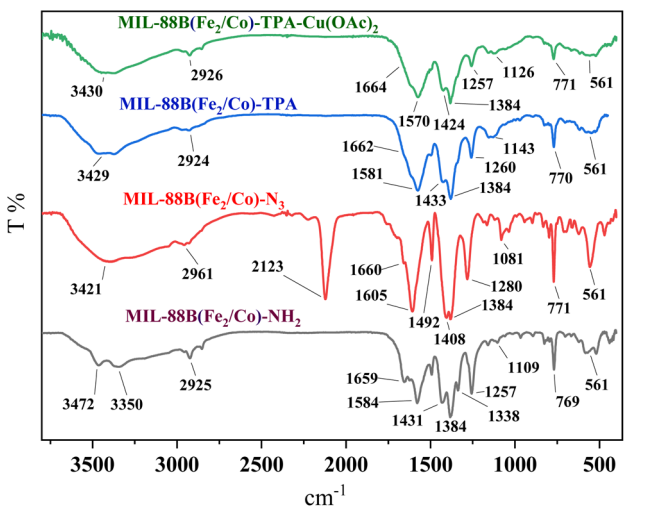

Fig. 5 FT-IR spectra of different stages synthesis of MIL-88B(Fe_2/Co)-TPA-Cu(OAc)$_2$ as an efficient porous catalyst containing copper complex based on Fe and Co-based bimetallic-MOFs.

^{1}H-NMR and ^{13}C-NMR techniques (see SI and spectral data section).

Various techniques were used to prove the structure of the prepared catalyst. FT-IR technique according to the results of Fig. 5 was used to identify functional groups in the structure of different stages of catalyst synthesis. The presence of the carbonyl group in the structure of MIL-88B(Fe_2/Co)-NH_2 was proved by observing the peak of 1659 cm^{-1} that this group is involved with the metals. The NH_2 group was well observed in the 3472 and 3350 cm^{-1} regions. Also, the two peaks in the 550–775 cm^{-1} regions show the presence of Fe–O and Co–O bonds. The results are consistent with the previously reported data.[50,52] In the next step, the removal of the amine group and the addition of the peak at the 2123 cm^{-1} region confirm the presence of the N_3 group. Removal of the azide group proves the formation of the triazole ring and the addition of copper acetate in later stages according to the spectra in Fig. 5. The results clearly show that the desired functional groups are well established in the structure of each step of the catalyst synthesis.

The morphology of each structure is proved by using the scanning electron microscope (SEM) technique. The morphology of the MIL-88B(Fe_2/Co)-NH_2 has appeared as a spindle-shaped structure according to the images in Fig. 6. This spindle-shaped morphology did not disappear and remained constant after various stages of functionalization and synthesis of the final catalyst, which indicates its proper stability.

X-ray powder diffraction analysis (XRD) is one of the best analyses to check the growth of crystal plates of the compounds. The XRD technique was used to investigate the growth pattern of crystal plates of the structure MIL-88B(Fe_2/Co)-TPA-Cu$(OAc)_2$ as an efficient porous catalyst (Fig. 7). The crystal sheet pattern of the MIL-88B(Fe_2/Co)-NH_2 structure agrees with the previous reports,[50,52] and it also bears a good resemblance to its simulated counterpart.[59] This pattern has remained well fixed in the later stages and the main peaks indicating the formation of MOF have appeared in all stages. The stability of the crystal plates of each structure shows its stability, which is well observed in the structure of the catalyst in question.

In another study, the presence of constituent elements of each structure was investigated using energy dispersive X-ray (EDX) analysis. The results can be seen in Fig. 8. The elements iron, cobalt, nitrogen, oxygen and carbon are shown in Fig. 8a and agree on the structure of MIL-88B(Fe_2/Co)-NH_2. In the structure of MIL-88B(Fe_2/Co)-TPA-Cu$(OAc)_2$ as an efficient porous catalyst, in addition to the mentioned elements, the presence of copper element can also be seen in Fig. 8b. Also, the uniform dispersion of elements in the final catalyst has been proven according to Fig. 8c and d. This issue is determined according to the elemental mapping analysis, which confirms the results of the EDX analysis.

In another search, the textural properties of MIL-88B(Fe_2/Co)-TPA-Cu$(OAc)_2$ as an efficient porous catalyst were studied by N_2 adsorption–desorption isotherms (Fig. 9a). Based on the obtained results, the area was calculated based on the BET equation and the total pore volume was 11.798 m^2 g^{-1} and 0.0979 cm^3 g^{-1} respectively. The pore size distribution of MIL-

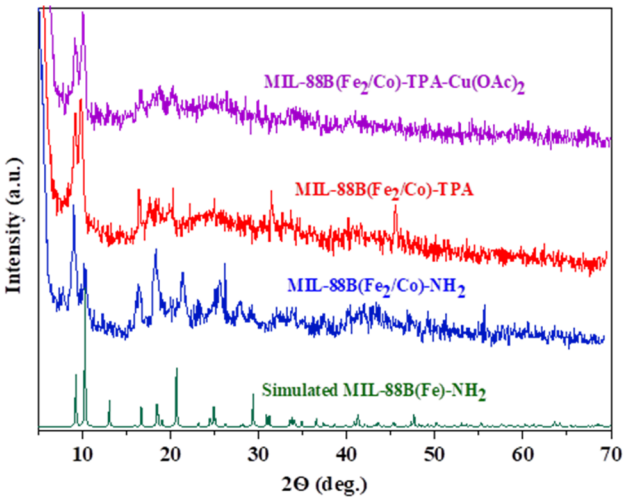

Fig. 7 Comparison of XRD patterns of different stages of synthesis MIL-88B(Fe_2/Co)-TPA-Cu$(OAc)_2$ as an efficient porous catalyst containing copper complex based on Fe and Co-based bimetallic-MOFs.

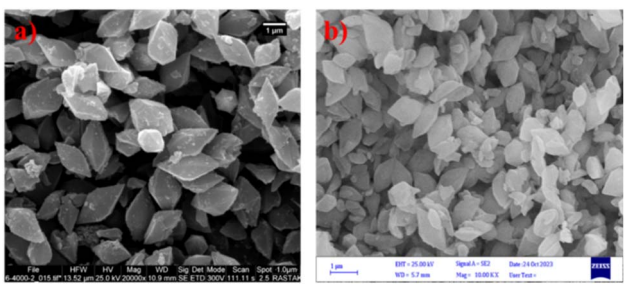

Fig. 6 Scanning electron microscope (SEM) images of (a) MIL-88B(Fe_2/Co)-NH_2 and (b) MIL-88B(Fe_2/Co)-TPA-Cu$(OAc)_2$ as an efficient porous catalyst containing copper complex based on Fe and Co-based bimetallic-MOFs.

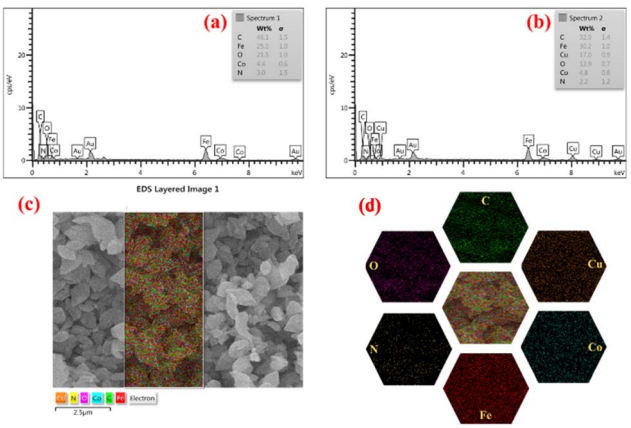

Fig. 8 Energy-dispersive X-ray spectroscopy (a) MIL-88B(Fe_2/Co)-NH_2 (b) MIL-88B(Fe_2/Co)-TPA-Cu$(OAc)_2$ and (c and d) elemental mapping analysis of MIL-88B(Fe_2/Co)-TPA-Cu$(OAc)_2$ as an efficient porous catalyst containing copper complex based on Fe and Co-based bimetallic-MOFs.

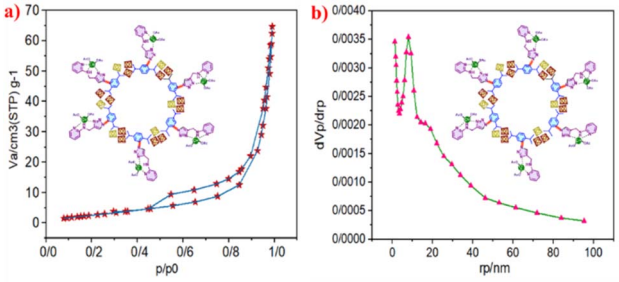

Fig. 9 (a) N_2 adsorption–desorption isotherms and (b) the pore size distribution of MIL-88B(Fe_2/Co)-TPA-Cu(OAc)$_2$ as an efficient porous catalyst containing copper complex based on Fe and Co-based bimetallic-MOFs.

88B(Fe_2/Co)-TPA-Cu(OAc)$_2$ as an efficient porous catalyst based on the BJH method is shown in (Fig. 9b). The mean pore diameter for the catalyst is 7.99 nm. The presence of a suitable surface area as well as the size of catalyst cavities can be a major reason for the synthesis of new phenylnicotinonitriles with high efficiency.

The proof of the thermal stability of each structure is using thermal gravimetric (TGA) and derivative thermal gravimetric (DTG) analysis. This analysis was taken from the structure of MIL-88B(Fe_2/Co)-TPA-Cu(OAc)$_2$ as an efficient porous catalyst and the results are shown in Fig. 10. According to the obtained results, several failures can be seen in the diagram, which can be due to the separation of different parts from the catalyst. The main failure is observed at the temperature of 280 °C, which shows that the catalyst can be used for catalyst purposes up to this temperature.

X-ray photoelectron spectroscopy (XPS) was used to confirm the chemical composition of MIL-88B(Fe_2/Co)-TPA-Cu(OAc)$_2$ as an efficient porous catalyst. The XPS survey spectra showed the presence of copper, iron, cobalt, oxygen, carbon, and nitrogen in the synthesized catalyst and peaks corresponding to Cu 2p, Fe 2p, Co 2p, O 1s, C 1s; and N 1s were detected (Fig. 11a-survey

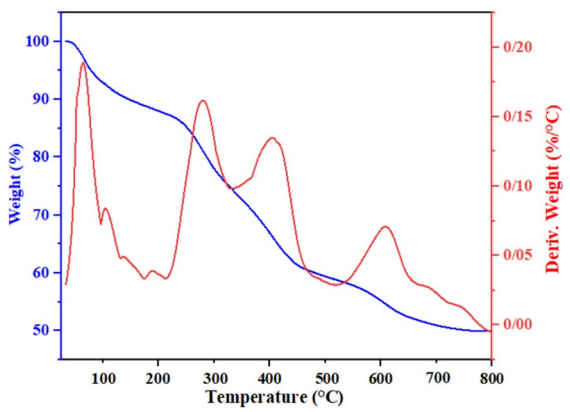

Fig. 10 Thermal gravimetric (TGA) and derivative thermal gravimetric (DTG) analysis of MIL-88B(Fe_2/Co)-TPA-Cu(OAc)$_2$ as an efficient porous catalyst containing copper complex based on Fe and Co-based bimetallic-MOFs.

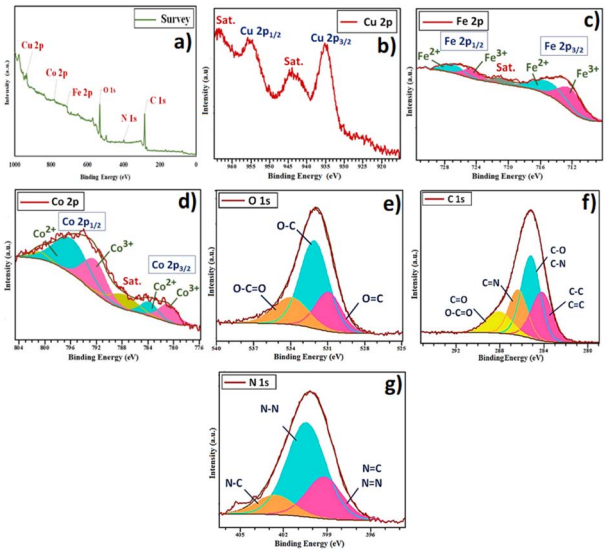

Fig. 11 The X-ray photoelectron spectroscopy (XPS) of MIL-88B(Fe_2/Co)-TPA-Cu(OAc)$_2$ as an efficient porous catalyst: (a) survey spectrum, (b) Cu 2p, (c) Fe 2p, (d) Co 2p, (e) O 1s, (f) C 1s and (g) N 1s.

spectrum). The high-resolution XPS spectrum of Cu(2p) shows two peaks at the binding energy of 936.2 and 956.7 eV, which belong to Cu $2p_{3/2}$ and Cu $2p_{1/2}$, respectively (Fig. 11b). The high-resolution XPS spectrum of Fe(2p) shows two peaks at the binding energy of 712.1 and 724.3 eV, which belong to Fe $2p_{3/2}$ and Fe $2p_{1/2}$, respectively (Fig. 11c). The high-resolution XPS spectrum of Co(2p) shows two peaks at the binding energy of

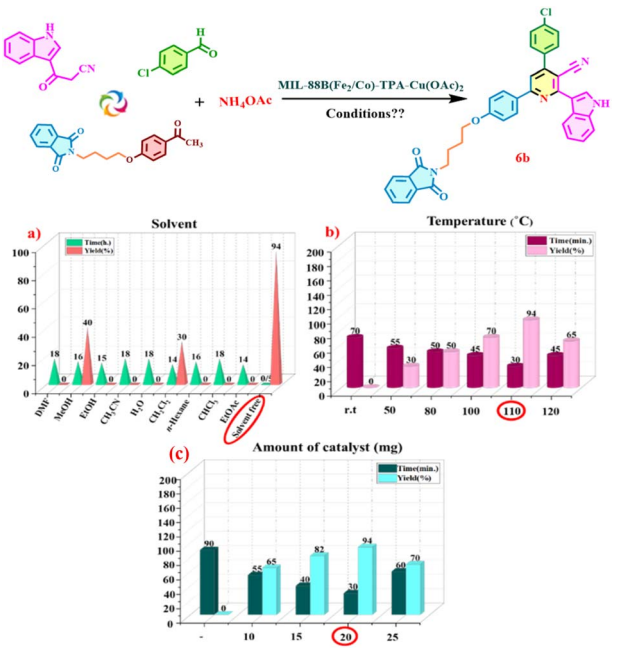

Fig. 12 Optimization some of the reaction's parameters using MIL-88B(Fe_2/Co)-TPA-Cu(OAc)$_2$ as an efficient porous catalyst containing copper complex based on Fe and Co-based bimetallic-MOFs: (a) solvent (b) temperature and (c) amount of catalyst.

Table 1 Synthesis of a new class of phenylnicotinonitriles using MIL-88B(Fe_2/Co)-TPA-$Cu(OAc)_2$ as an efficient porous catalyst containing copper complex based on Fe and Co-based bimetallic-MOFs

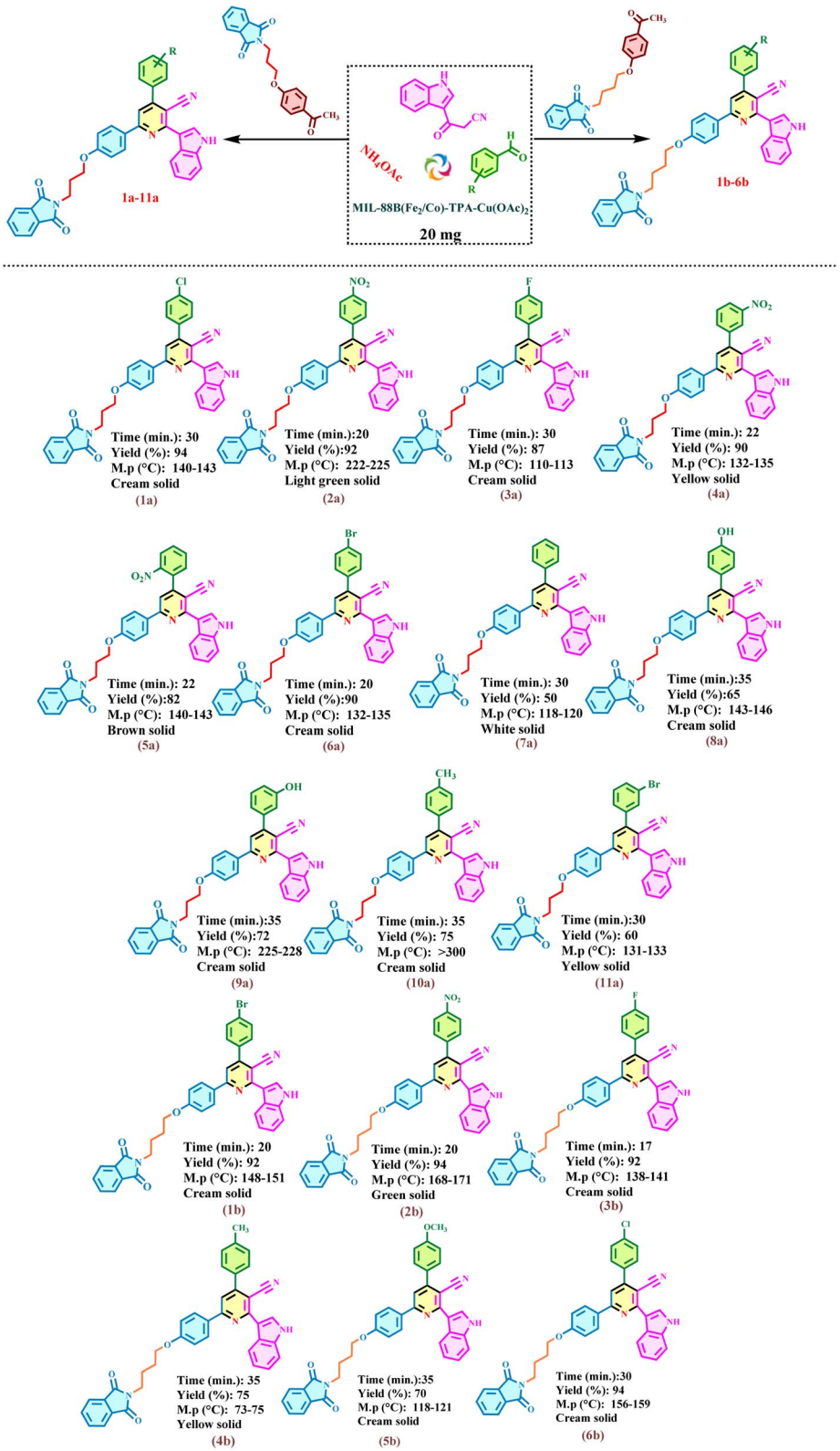

780.8 and 792.6 eV, which belong to Co $2p_{3/2}$ and Co $2p_{1/2}$, respectively (Fig. 11d). The high-resolution XPS spectrum of O 1s showed three peaks in the regions of 531.2, 532.3 and 534.3 eV, which are related to O=C, O–C and O–C=O species (Fig. 11e). The O-metal species overlapped in these regions. The high-resolution XPS spectrum of C 1s showed four peaks in the

regions of 284.2, 285.3, 286.7 and 288.6 eV, which are related to C–C/C=C, C–N/C–O, C=N and C=O/O–C=O species (Fig. 11f). The high-resolution XPS spectrum of N1s showed three broad peaks in the regions of 399.5, 400.2 and 402.5 eV, which are related to N=C, N=N, N–N and N–C species (Fig. 11g).[8,60] The N–Cu species overlapped in these regions. The results obtained confirm the structure well.

After confirming the structure of the catalyst using different techniques, the proof of its catalytic activity in the synthesis of a new class phenylnicotinonitriles was investigated. To optimize the reaction conditions, the reaction between 4-chlorobenzaldehyde (1 mmol, 0.140 g), 2-(4-(4-acetylphenoxy)propyl) isoindoline-1,3-dione (1 mmol, 0.337 g) and 3-(1*H*-indol-3-yl)-3-oxopropanenitrile (1 mmol, 0.184 g) was chosen as the model reaction. This reaction was investigated within the different solvents and also solvent-free conditions. According to the obtained results the solvent-free condition was chosen for the abovementioned reaction (Fig. 12a). Then, the model reaction was evaluated under different temperatures and amounts of catalyst (Fig. 12b and c). After checking various reaction conditions, the solvent-free at the 110 °C and amount of 20 mg of catalyst are the best choice. Thus, these conditions were chosen as optimal reaction conditions so that other derivatives can be synthesized under these conditions.

After determining the optimal conditions, application of the MIL-88B(Fe_2/Co)-TPA-Cu(OAc)$_2$ as an efficient porous catalyst for the synthesis of a new class of phenylnicotinonitriles was investigated. In order to achieve this goal, in optimal

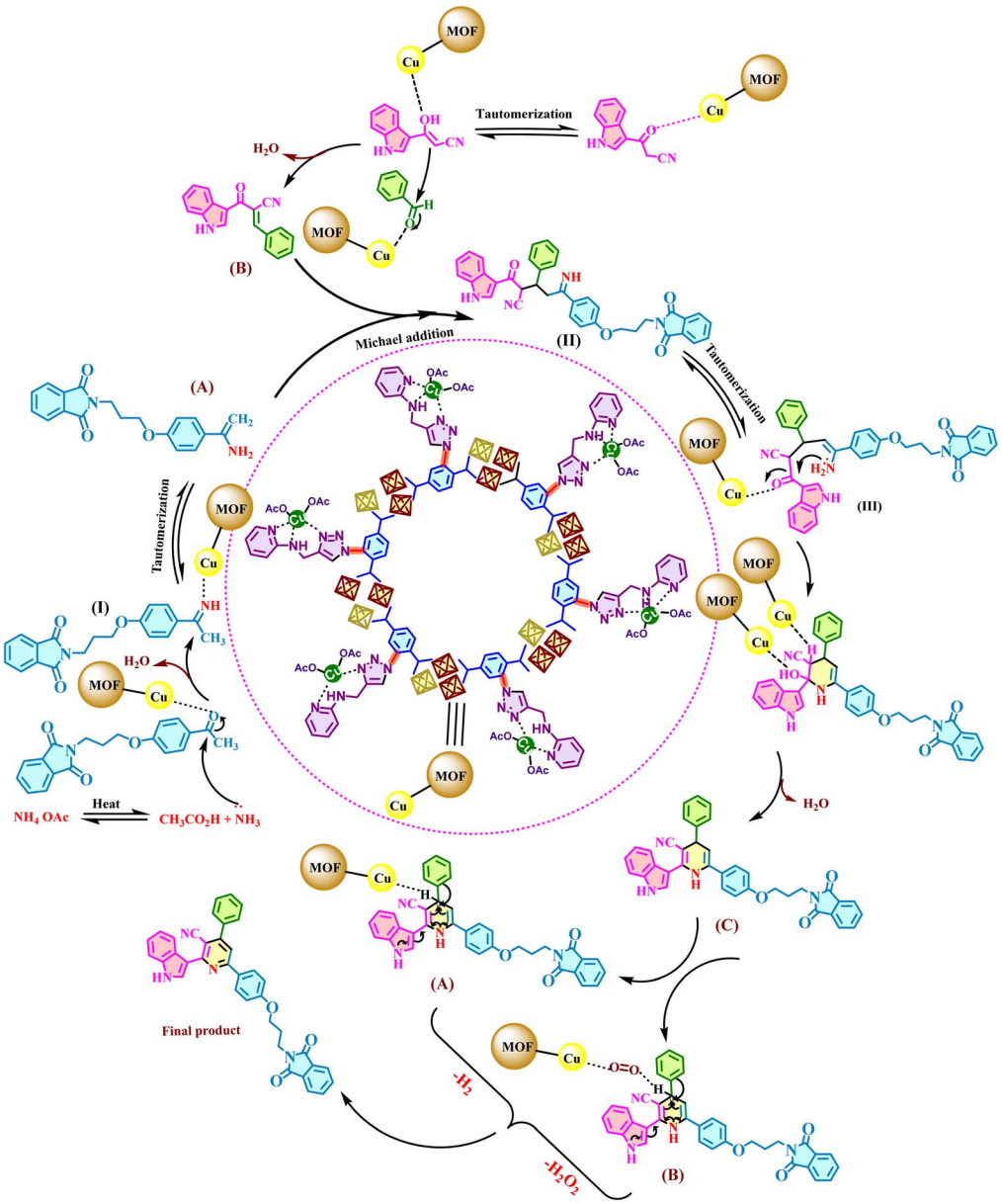

Scheme 3 The proposed mechanism for the synthesis of new phenylnicotinonitriles using MIL-88B(Fe_2/Co)-TPA-Cu(OAc)$_2$ as an efficient porous catalyst containing copper complex based on Fe and Co-based bimetallic-MOFs.

Table 2 Synthesis of new phenylnicotinonitriles in the presence of various catalysts

Entry	Catalyst	Amount of catalyst	Time (min.)	Yield (%)
1	MIL-88B(Fe_2/Co)-TPA-Cu$(OAc)_2$ (this work)	20 mg	30	94
2	MIL-88B(Fe_2/Co)-TPA (this work)	20 mg	30	55
3	MIL-88B(Fe_2/Co)-NH_2 (this work)	20 mg	30	40
4	$Cu(OAc)_2$	20 (mol%)	120	55
5	MOF(Fe)-TUR	20 mg	40	Trace
6	*p*-TSA	20 (mol%)	30	70
7	Zr-UiO-66-PDC$(CH_2)_4$-SO_3 (ref. 69)	20 mg	50	35
8	SSA[70]	20 mg	45	40
9	H_2SO_4	20 (mol%)	60	—
10	$N(Et)_3$	20 (mol%)	30	50
11	CQDs-N$(CH_2PO_3H_2)_2$ (ref. 4)	20 mg	55	60
12	MIL(100)(Cr)/NHEtN$(CH_2PO_3H_2)_2$ (ref. 71)	20 mg	30	60
13	[PVI-SO_3H]Cl[72]	20 mg	70	—
14	UiO-66-NH_2/melamine/[$N(CH_2PO_3H_2)_2$] (ref. 73)	20 mg	40	30
15	Pipyridine	20 (mol%)	30	Trace
16	CQD-N$(H_2PO_3)_2$/SBA15 (ref. 5)	20 mg	35	60

conditions, various benzaldehyde derivatives and compounds B and C (see in Scheme 2) were used for the synthesis of a wide range of the desired compounds. The results are shown in Table 1. According to the obtained results, the catalyst has shown this performance well and all the compounds have been synthesized in mild and green conditions. The structures of the synthesized products were evaluated and confirmed by melting point, FT-IR, ^{1}H-NMR and ^{13}C-NMR techniques (see in SI and spectral data section).

The proposed mechanism for the synthesis of new phenylnicotinonitriles is shown in Scheme 3. In the first step, the intermediate I is introduced *via* a reaction between the activated ketone and the *in situ* generated ammonia from ammonium acetate by losing the H_2O molecule. The intermediate I is converted to the Y-conjugated intermediate A through a tautomerization.[61–64] On the other hand, 3-(1*H*-indol-3-yl)-3-oxopropanenitrile is converted into an enolate form using a catalyst and reacts with aldehyde activated by the catalyst to create intermediate B by losing the H_2O molecule. Intermediate A reacts with intermediate B during nucleophilic attack and Michael addition to form intermediate (II). Intermediate (II) is converted to the intermediate (III) through a tautomerization. This intermediate is converted to intermediate C through intramolecular cyclization and the removal of one molecule of H_2O. Finally, the intermediate (III) converts to its corresponding derivative *via* a cooperative vinylogous anomeric based oxidation and releases one molecule of hydrogen ($-H_2$) and/or hydrogen peroxide ($-H_2O_2$) molecules.[65–68] The different categories of anomeric based oxidation have been mini-revied.[57,58] The term cooperative is used when more than one lone pair of electrons and other donors are sharing into an anti-bonding orbital of one acceptor bond ($n_N \rightarrow \sigma^*_{C-H}$). The simultaneous cooperative sharing of electrons from donors into the anti-bonding orbitals of the C–H bond is a major driving force for hydride releasing ($n_N \rightarrow \sigma^*_{C-H}$).

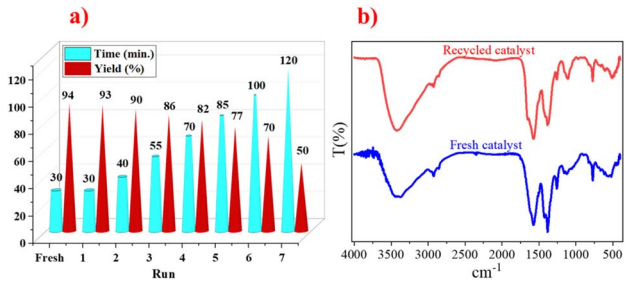

Fig. 13 (a) Reusability of MIL-88B(Fe_2/Co)-TPA-Cu $(OAc)_2$ as an efficient porous catalyst containing copper complex based on Fe and Co-based bimetallic-MOFs. (b) FT-IR for the recycled and fresh catalyst.

Catalyst efficiency becomes more important when compared to other catalysts. In this direction, to further investigate the efficiency of the desired catalyst, the model reaction was investigated under optimal conditions with other organic, inorganic, heterogeneous and homogeneous catalysts. The results of these tests are shown in Table 2. The results show that this reaction in the presence of MIL-88B(Fe_2/Co)-TPA-Cu$(OAc)_2$ as a catalyst has better conditions in terms of reaction time and product yield. Recycling and reusability of a catalyst can be economically and environmentally important. This property of MIL-88B(Fe_2/Co)-TPA-Cu$(OAc)_2$ as a presented catalyst was also investigated. The obtained results are collected in Fig. 13a. The results show that the catalyst can be reused up to 7 times with little change in product yield. To prove the stability of the catalyst, the FT-IR spectrum was taken from the recycled catalyst and compared to the freshly prepared catalyst, it is shown in Fig. 13b. According to this spectrum, the functional groups of the catalyst are well preserved after reuse and recycling.

4. Conclusion

In summary, the copper complex based on Fe and Co-based bimetallic-MOFs was designed and synthesized. In this porous catalyst, copper was fixed as a new porous complex on the surface of bimetallic metal–organic frameworks. The structure of the synthesized catalyst was identified and confirmed using FT-IR, XRD, SEM, EDX, Elemental mapping, XPS, BET/BJH and

TGA/DTG techniques. The catalytic activity of MIL-88B(Fe_2/Co)-TPA-Cu$(OAc)_2$ was evaluated in the synthesis of new phenylnicotinonitriles. It seems that these compounds have biological and medicinal applications due to the presence of biological cores such as indole, phthalimide, pyridine, *etc.* The structure of the synthesized products was investigated with their melting points, FT-IR, ^{1}H-NMR and ^{13}C-NMR techniques. In the proposed mechanism, it was observed that the cycle of pyridine proceeds through a cooperative vinylogous anomeric based oxidation. The stability and appropriate morphology of the presented catalyst can create a new approach in the preparation of porous and heterogeneous catalysts. High product efficiency and mild green conditions are other characteristics of products synthesized using this porous catalyst. Also, the results showed that the catalyst had good recyclability, which is very important in the synthesis of heterogeneous catalysts.

Author contributions

In terms appropriate to the academic context, the main experiments were conceived and performed by M. F.; and M. M. R. The ideas and main manuscript were written by H. S. The revision of the article and supervision of the study were guided by M. A. Z.; and M. H.

Conflicts of interest

There are no conflicts to declare.

Data availability

All data supporting this study has been included in the SI.

Spectral data of the new phenylnicotinonitriles such as FT-IR, ^{1}H-NMR and ^{13}C-NMR spectra of the synthesized derivatives. See DOI: **https://doi.org/10.1039/d5ra04067a**.

Acknowledgements

We thank Bu-Ali Sina University for financial support this research.

References

1 F. Khosravi, M. Gholinejad, J. M. Sansano and R. Luque, Low-amount palladium supported on Fe-Cu MOF: Synergetic effect between Pd, Cu and Fe in Sonogashira-Hagihara coupling reaction and reduction of organic dyes, *Mol. Catal.*, 2022, **522**, 112199.

2 Z. Weng, Y. Wu, M. Wang, J. Jiang, K. Yang, S. Huo, X. F. Wang, Q. Ma, G. W. Brudvig, V. S. Batista and Y. Liang, Active sites of copper-complex catalytic materials for electrochemical carbon dioxide reduction, *Nat. Commun.*, 2018, **9**, 415.

3 N. Naz, M. H. Manzoor, S. M. G. Naqvi, U. Ehsan, M. Aslam and F. Verpoort, Porous organic polymers; an emerging material applied in energy, environmental and biomedical applications, *Appl. Mater. Today*, 2024, **38**, 102198.

4 M. M. Rasooll, M. Zarei, M. A. Zolfigol, H. Sepehrmansourie, A. Omidi, M. Hasani and Y. Gu, Novel nano-architectured carbon quantum dots (CQDs) with phosphorous acid tags as an efficient catalyst for the synthesis of multisubstituted 4 H-pyran with indole moieties under mild conditions, *RSC Adv.*, 2021, **11**, 25995–26007.

5 M. M. Rasooll, H. Sepehrmansourie, M. Zarei, M. A. Zolfigol and S. Rostamnia, Phosphonic acid tagged carbon quantum dots encapsulated in SBA-15 as a novel catalyst for the preparation of *N*-heterocycles with pyrazolo, barbituric acid and indole moieties, *Sci. Rep.*, 2022, **12**, 20812.

6 F. Jalili, M. Zarei, M. A. Zolfigol, S. Rostamnia and A. R. Moosavi-Zare, SBA-15/PrN $(CH_2PO_3H_2)_2$ as a novel and efficient mesoporous solid acid catalyst with phosphorous acid tags and its application on the synthesis of new pyrimido [4,5-*b*] quinolones and pyrido [2, 3-*d*] pyrimidines via anomeric based oxidation, *Microporous Mesoporous Mater.*, 2020, **294**, 109865.

7 S. Kalhor, M. Zarei, M. A. Zolfigol, H. Sepehrmansourie, D. Nematollahi, S. Alizadeh, H. Shi and J. Arjomandi, Anodic electrosynthesis of MIL-53(Al)-N$(CH_2PO_3H_2)_2$ as a mesoporous catalyst for synthesis of novel (*N*-methylpyrrol)-pyrazolo[3,4-*b*] pyridines via a cooperative vinylogous anomeric based oxidation, *Sci. Rep.*, 2021, **11**, 19370.

8 E. Tavakoli, H. Sepehrmansourie, M. A. Zolfigol, A. Khazaei, A. Mohammadzadeh, E. Ghytasranjbar and M. A. As' Habi, Synthesis and application of task-specific bimetal–organic frameworks in the synthesis of biological active spirooxindoles, *Inorg. Chem.*, 2024, **63**, 5805–5820.

9 S. Kalhor, H. Sepehrmansourie, M. Zarei, M. A. Zolfigol and H. Shi, Application of functionalized Zn-based metal–organic frameworks (Zn-MOFs) with CuO in heterocycle synthesis via azide–alkyne cycloaddition, *Inorg. Chem.*, 2024, **63**, 4898–4914.

10 H. Sepehrmansourie, M. Zarei, M. Mohammadi Rasooll, M. A. Zolfigol and Y. Gu, Application of metal–organic frameworks with sulfonic acid tags in the synthesis of pyrazolo [3, 4-*b*] pyridines via a cooperative vinylogous anomeric-based oxidation, *Inorg. Chem.*, 2023, **62**, 9217–9229.

11 S. Kalhor, M. Zarei, H. Sepehrmansourie, M. A. Zolfigol, H. Shi, J. Wang, J. Arjomandi, M. Hasani and R. Schirhagl, Novel uric acid-based nano organocatalyst with phosphorous acid tags: Application for synthesis of new biologically-interest pyridines with indole moieties via a cooperative vinylogous anomeric based oxidation, *Mol. Catal.*, 2021, **507**, 111549.

12 J. Afsar, M. A. Zolfigol, A. Khazaei, M. Zarei, Y. Gu, D. A. Alonso and A. Khoshnood, Synthesis and application of melamine-based nano catalyst with phosphonic acid tags in the synthesis of (3-indolyl) pyrazolo [3, 4-*b*] pyridines via vinylogous anomeric based oxidation, *Mol. Catal.*, 2020, **482**, 110666.

13 B. Danishyar, H. Sepehrmansourie, M. Zarei, M. A. Zolfigol, M. A. As' Habi and Y. Gu, Synthesis and application of novel magnetic glycoluril tetrakis (methylene phosphorous acid)

as a nano biological catalyst for the preparation of nicotinonitriles via a cooperative vinylogous anomeric-based oxidation, *Polycycl. Aromat. Compd.*, 2023, **43**, 6837–6857.

14 M. Zarei, H. Sepehrmansourie, M. A. Zolfigol, R. Karamian and S. H. M. Farida, Novel nano-size and crab-like biological-based glycoluril with sulfonic acid tags as a reusable catalyst: Its application to the synthesis of new mono-and bis-spiropyrans and their in vitro biological studies, *New J. Chem.*, 2018, **42**, 14308–14317.

15 S. Moradi, M. A. Zolfigol, M. Zarei, D. A. Alonso and A. Khoshnood, Synthesis of a Biological-Based Glycoluril with Phosphorous Acid Tags as a New Nanostructured Catalyst: Application for the Synthesis of Novel Natural Henna-Based Compounds, *ChemistrySelect*, 2018, **3**, 3042–3047.

16 M. Torabi, M. Yarie, A. Tavassoli, N. Zarei, L. Vatannavaz, M. A. Zolfigol and S. Azizian, synthesis and applications, *Coord. Chem. Rev.*, 2025, **527**, 216359.

17 A. Jose, T. Mathew, N. Fernández-Navas and C. J. Querebillo, Porous Inorganic Nanomaterials: Their Evolution towards Hierarchical Porous Nanostructures, *Micro*, 2024, **4**, 229–280.

18 A. Wang, Y. Ma and D. Zhao, Pore engineering of Porous Materials: Effects and Applications, *ACS Nano*, 2024, **18**, 22829–22854.

19 B. Mohanty, S. Kumari, P. Yadav, P. Kanoo and A. Chakraborty, Metal-organic frameworks (MOFs) and MOF composites-based biosensors, *Coord. Chem. Rev.*, 2024, **519**, 216102.

20 I. E. Khalil, J. Fonseca, M. R. Reithofer, T. Eder and J. M. Chin, tackling orientation of metal-organic frameworks (MOFs): The quest to enhance MOF performance, *Coord. Chem. Rev.*, 2023, **481**, 215043.

21 T. De Villenoisy, X. Zheng, V. Wong, S. S. Mofarah, H. Arandiyan, Y. Yamauchi, P. Koshy and C. C. Sorrell, Principles of design and synthesis of metal derivatives from MOFs, *Adv. Mater.*, 2023, **35**, 2210166.

22 (*a*) X. Liu, Y. Shan, S. Zhang, Q. Kong and H. Pang, Application of metal organic framework in wastewater treatment, *Green Energy Environ.*, 2023, **8**, 698–721; (*b*) I. Letchumanan, A. A. Wani, N. Shaari, M. Beygisangchin, S. K. Kamarudin and N. A. Karim, Metal–Organic Frameworks as a Catalyst and Catalyst Support in Fuel Cells: From Challenges to Catalytic Application, *Chem. Eng. Technol.*, 2024, **47**, e202300580; (*c*) Y. Lu, H. Zhou, H. Yang, Z. Zhou, Z. Jiang and H. Pang, Anisotropy of metal–organic framework and their composites: properties, synthesis, and applications, *J. Mater. Chem. A*, 2024, **12**, 6243–6260.

23 D. Li, A. Yadav, H. Zhou, K. Roy, P. Thanasekaran and C. Lee, Advances and Applications of Metal-Organic Frameworks (MOFs) in Emerging Technologies: A Comprehensive Review, *Glob. Chall.*, 2024, **8**, 2300244.

24 Y. Deng, M. Guo, L. Zhou, Y. Huang, S. Srivastava, A. Kumar and J. Q. Liu, Prospects, advances and biological applications of MOF-based platform for the treatment of lung cancer, *Biomater. Sci.*, 2024, **12**, 3725–3744.

25 (*a*) H. Sepehrmansourie, H. Alamgholiloo, N. N. Pesyan and M. A. Zolfigol, A MOF-on-MOF strategy to construct double Z-scheme heterojunction for high-performance photocatalytic degradation, *Appl. Catal., B*, 2023, **321**, 122082; (*b*) H. Sepehrmansourie, H. Alamgholiloo, M. A. Zolfigol, N. N. Pesyan and M. M. Rasooll, Nanoarchitecting a dual Z-Scheme Zr-MOF/Ti-MOF/g-C_3N_4 heterojunction for boosting Gomberg–Buchmann–Hey reactions under visible light conditions, *ACS Sustain. Chem. Eng.*, 2023, **11**, 3182–3193.

26 A. Ebrahimi, L. Krivosudský, A. Cherevan and D. Eder, Polyoxometalate-based porphyrinic metal-organic frameworks as heterogeneous catalysts, *Coord. Chem. Rev.*, 2024, **508**, 215764.

27 G. Lin, B. Zeng, J. Li, Z. Wang, S. Wang, T. Hu and L. Zhang, A systematic review of metal organic frameworks materials for heavy metal removal: Synthesis, applications and mechanism, *Chem. Eng. J.*, 2023, **460**, 141710.

28 (*a*) J. Luo, X. Luo, Y. Gan, X. Xu, B. Xu, Z. Liu, C. Ding, Y. Cui and C. Sun, Advantages of bimetallic organic frameworks in the adsorption, catalysis and detection for water contaminants, *Nanomaterials*, 2023, **13**, 2194; (*b*) K. F. Kayani, Bimetallic metal–organic frameworks (BMOFs) for dye removal: a review, *RSC Adv.*, 2024, **14**, 31777–31796.

29 T. R. Katugampalage, P. Waribam, P. Opaprakasit, C. Kaewsaneha, S. H. Hsu, W. Chooaksorn, C. A. Jong, P. Sooksaen, C. Ratanatawanate and P. Sreearunothai, Bimetallic Fe: Co metal–organic framework (MOF) with unsaturated metal sites for efficient Fenton-like catalytic degradation of oxytetracycline (OTC) antibiotics, *Chem. Eng. J.*, 2024, **479**, 147592.

30 (*a*) M. I. Bashir, F. Anjum, M. Imran, H. M. Fahad and F. Sher, Facile synthesis of hybrid electrode by bimetallic MOFs/polyaniline composite for high-performance asymmetric supercapacitors, *J. Mater. Sci.: Mater. Electron.*, 2024, **35**, 742; (*b*) I. Saini, V. Singh and S. Hamad, Recent development in bimetallic metal organic frameworks as photocatalytic material, *Inorg. Chem. Commun.*, 2023, **160**, 111897.

31 G. Mohammad Abu-Taweel, S. S. Alharthi, H. M. Al-Saidi, A. O. Babalghith, M. M. Ibrahim and S. Khan, Heterocyclic organic compounds as a fluorescent chemosensor for cell imaging applications: a review, *Crit. Rev. Anal. Chem.*, 2024, **54**, 2538–2553.

32 M. Marinescu and C. V. Popa, Pyridine compounds with antimicrobial and antiviral activities, *Int. J. Mol. Sci.*, 2022, **23**, 5659.

33 R. Rossi and M. Ciofalo, An updated review on the synthesis and antibacterial activity of molecular hybrids and conjugates bearing imidazole moiety, *Molecules*, 2020, **25**, 5133.

34 S. M. Hassan, A. Farid, S. S. Panda, M. S. Bekheit, H. Dinkins, W. Fayad and A. S. Girgis, Indole compounds in oncology:

therapeutic potential and mechanistic insights, *Pharmaceuticals*, 2024, **17**, 922.

35 M. R. Elmorsy, S. E. Mahmoud, A. A. Fadda, E. Abdel-Latif and M. A. Abdelmoaz, Synthesis, biological evaluation and molecular docking of new triphenylamine-linked pyridine, thiazole and pyrazole analogues as anticancer agents, *BMC Chem.*, 2022, **16**, 88.

36 M. L. Almeida, M. C. Oliveira, I. R. Pitta and M. G. Pitta, Advances in synthesis and medicinal applications of compounds derived from phthalimide, *Curr. Org. Synth.*, 2020, **17**, 252–270.

37 H. A. Hamid, A. N. Ramli and M. M. Yusoff, Indole alkaloids from plants as potential leads for antidepressant drugs: A mini review, *Front. Pharmacol.*, 2017, **8**, 96.

38 H. M. Abd El-Lateef, M. M. Khalaf, M. Gouda, M. Kandeel, A. A. Amer, A. A. Abdelhamid and M. A. Gad, Functionalized pyridines: Synthesis and toxicity evaluation of potential insecticidal agents against Aphis craccivora, *ACS Omega*, 2023, **8**, 29685–29692.

39 S. Sharma and S. Singh, The biological and pharmacological potentials of indole-based heterocycles, *Lett. Org. Chem.*, 2023, **20**, 711–729.

40 I. V. Alabugin, *Stereoelectronic Effects: A Bridge between Structure and Reactivity*, JWS, 1st edn, 2016.

41 E. M. Pérez, E. Matamoros, P. Cintas and J. C. Palacios, Exploring and Re-Assessing Reverse Anomeric Effect in 2-Iminoaldoses Derived from Mono-and Polynuclear Aromatic Aldehydes, *Molecules*, 2024, **29**, 4131.

42 I. V. Alabugin, L. Kuhn, M. G. Medvedev, N. V. Krivoshchapov, V. A. Vil, I. A. Yaremenko, P. Mehaffy, M. Yarie, A. O. Terent'ev and M. A. Zolfigol, Stereoelectronic power of oxygen in control of chemical reactivity: the anomeric effect is not alone, *Chem. Soc. Rev.*, 2021, **50**, 10253.

43 V. Alabugin, L. Kuhn, N. V. Krivoshchapov, P. Mehaffy and M. G. Medvedev, Anomeric effect, hyperconjugation and electrostatics: Lessons from complexity in a classic stereoelectronic phenomenon, *Chem. Soc. Rev.*, 2021, **50**, 10212.

44 (*a*) J. T. Edward, *Chem. Ind.*, 1955, 1102–1104; (*b*) E. Juaristi and G. Cuevas, Recent studies of the anomeric effect, *Tetrahedron*, 1992, **48**, 5019–5087.

45 (*a*) C. B. Bai, N. X. Wang, Y. Xing and X. W. Lan, Progress on chiral NAD(P)H model compounds, *Synlett*, 2017, **28**, 402–414; (*b*) G. Hamasaka, H. Tsuji and Y. Uozumi, Organoborane-catalyzed hydrogenation of unactivated aldehydes with a Hantzsch ester as a synthetic NAD(P)H analogue, *Synlett*, 2015, **26**, 2037–2041.

46 H. Sepehrmansourie, M. Zarei, M. A. Zolfigol and Y. Gu, A new approach for the synthesis of bis (3-Indolyl) pyridines via a cooperative vinylogous anomeric based oxidation using ammonium acetate as a dual reagent-catalyst role under mild and green condition, *Polycycl. Aromat. Compd.*, 2023, **43**, 6998–7012.

47 H. Ahmadi, M. Zarei and M. A. Zolfigol, Catalytic application of a novel basic alkane-sulfonate metal-organic frameworks in the preparation of pyrido[2,3-*d*]pyrimidines via a cooperative vinylogous anomeric-based oxidation, *ChemistrySelect*, 2022, **7**, e202202155.

48 H. Sepehrmansourie, M. Zarei, M. A. Zolfigol, S. Babaee, S. Azizian and S. Rostamnia, Catalytic synthesis of new pyrazolo [3, 4-*b*] pyridine via a cooperative vinylogous anomeric-based oxidation, *Sci. Rep.*, 2022, **12**, 14145.

49 M. M. Rasooll, H. Sepehrmansourie, M. Zarei, M. A. Zolfigol, M. Hosseinifard and Y. Gu, Catalytic Application of Functionalized Bimetallic–Organic Frameworks with Phosphorous Acid Tags in the Synthesis of Pyrazolo [4, 3-*e*] pyridines, *ACS Omega*, 2023, **8**, 25303–25315.

50 M. M. Rasooll, H. Sepehrmansourie, M. A. Zolfigol, M. Hosseinifard, S. L. Hosseini and Y. Gu, Application of a new porous bimetallic H-bond catalyst in the preparation of biological henna-based pyrazolo [3, 4-*b*] quinolines via a cooperative vinylogous anomeric based oxidation, *Mol. Catal.*, 2025, **570**, 114628.

51 M. A. Zolfigol, S. Azizian, M. Torabi, M. Yarie and B. Notash, The Importance of Nonstoichiometric Ratio of Reactants in Organic Synthesis, *J. Chem. Educ.*, 2024, **101**, 877–881.

52 B. Iqbal, M. Saleem, S. N. Arshad, J. Rashid, N. Hussain and M. Zaheer, One-pot synthesis of heterobimetallic metal–organic frameworks (MOFs) for multifunctional catalysis, *Chem.–Eur. J.*, 2019, **25**, 10490–10498.

53 B. Negi, D. Kumar, W. Kumbukgolla, S. Jayaweera, P. Ponnan, R. Singh, S. Agarwal and D. S. Rawat, Anti-methicillin resistant Staphylococcus aureus activity, synergism with oxacillin and molecular docking studies of metronidazole-triazole hybrids, *Eur. J. Med. Chem.*, 2016, **115**, 426–437.

54 E. M. Rodríguez, N. Bogdan, J. A. Capobianco, S. Orlandi, M. Cavazzini, C. Scalera and S. A. Quici, A highly sensitive luminescent lectin sensor based on an *α*-*d*-mannose substituted Tb^{3+} antenna complex, *Dalton Trans.*, 2013, **42**, 9453–9461.

55 Z. Torkashvand, H. Sepehrmansourie, M. A. Zolfigol and Y. Gu, Ti-based MOFs with acetic acid pendings as an efficient catalyst in the preparation of new spiropyrans with biological moieties, *Sci. Rep.*, 2024, **14**, 14101.

56 R. M. Abdel-Motaleb, A. M. A. S. Makhloof, H. M. Ibrahim and M. H. Elnagdi, Studies with azoles and benzoazoles: A novel simple approach for synthesis of 3-functionally substituted 3-acylindoles, *J. heterocycl. Chem.*, 2007, **44**, 109–114.

57 M. Yarie, Catalytic anomeric based oxidation, *Iran. J. Catal.*, 2017, **7**, 85–88.

58 M. Yarie, Catalytic vinylogous anomeric based oxidation (Part I), *Iran. J. Catal.*, 2020, **10**, 79–83.

59 (*a*) J. Wang, J. Wang, M. Zhang, S. Li, R. Liu and Z. Li, Metalorganic frameworks-derived hollow-structured iron-cobalt bimetallic phosphide electrocatalysts for efficient oxygen evolution reaction, *J. Alloys Compd.*, 2020, **821**, 153463; (*b*) S. Bauer, C. Serre, T. Devic, P. Horcajada, J. Marrot, G. Ferey and N. Stock, High-throughput assisted rationalization of the formation of metal organic frameworks in the iron (III) amino terephthalate solvothermal system, *Inorg. Chem.*, 2008, **47**, 7568–7576.

60 (*a*) R. Zandipak, N. Bahramifar, H. Younesi and M. A. Zolfigol, Electro-photocatalyst effect of NS-doped carbon dots and covalent organic triazine framework heterostructures for boosting photocatalytic degradation of phenanthrene in water, *Chemosphere*, 2024, **364**, 142980; (*b*) R. Zandipak, N. Bahramifar, H. Younesi and M. A. Zolfigol, Decoration of carbon nanodots on conjugated triazine framework nanosheets as Z-scheme heterojunction for boosting opto-electro photocatalytic degradation of organic hydrocarbons from petrochemical wastewater, *J. Environ. Chem. Eng.*, 2025, **13**, 115380.

61 P. Gund, Guanidine, trimethylolethane., and "Y-delocalization". Can acyclic compounds have "aromatic" stability?, *J. Chem. Educ.*, 1972, (49), 100.

62 N. J. Head, G. A. Olah and G. S. Prakash, (Hexaphenyltrimethylene) methane dication and related carbocations, *J. Am. Chem. Soc.*, 1995, **117**, 11205–11210.

63 T. Ohwada, H. Kagawa and H. Ichikawa, π-Conjugation in Y-Shaped Configuration. Does a Special Stability Exist?, *Bull. Chem. Soc. Jpn.*, 1997, **70**, 2411–2415.

64 E. Kleinpeter and A. Koch, *Y*-aromaticity–existing: yes, or no? An answer given on the magnetic criterion (TSNMRS), *Tetrahedron*, 2016, **72**, 1675–1685.

65 M. Navazeni, M. A. Zolfigol, H. Ahmadi, H. Sepehrmansourie, A. Khazaei and M. Hosseinifard, Design, synthesis and application of a magnetic H-bond catalyst in the preparation of new nicotinonitriles via cooperative vinylogous anomeric-based oxidation, *RSC Adv.*, 2024, **14**, 16607–16616.

66 E. Tavakoli, H. Sepehrmansourie, M. Zarei, M. A. Zolfigol, A. Khazaei and M. A. As' Habi, Application of Zr-MOFs based copper complex in synthesis of pyrazolo [3, 4-*b*] pyridine-5-carbonitriles via anomeric-based oxidation, *Sci. Rep.*, 2023, **13**, 9388.

67 B. Danishyar, H. Sepehrmansourie, H. Ahmadi, M. Zarei, M. A. Zolfigol and M. Hosseinifard, Application of nanomagnetic metal–organic frameworks in the green synthesis of nicotinonitriles via cooperative vinylogous anomeric-based oxidation, *ACS Omega*, 2023, **8**, 18479–18490.

68 S. Babaee, M. Zarei and M. A. Zolfigol, Synthesis of picolinates via a cooperative vinylogous anomeric-based oxidation using UiO-66 (Zr)-*N* $(CH_2\ PO_3\ H_2)_2$ as a catalyst, *RSC Adv.*, 2021, **11**, 36230–36236.

69 A. M. Naseri, M. Zarei, S. Alizadeh, S. Babaee, M. A. Zolfigol, D. Nematollahi and H. Shi, Synthesis and application of [Zr-UiO-66-PDC-SO_3H] Cl MOFs to the preparation of dicyanomethylene pyridines via chemical and electrochemical methods, *Sci. Rep.*, 2021, **11**, 16817.

70 (*a*) M. A. Zolfigol, Silica sulfuric acid/$NaNO_2$ as a novel heterogeneous system for production of thionitrites and disulfides under mild conditions, *Tetrahedron*, 2001, **57**, 9509–9511; (*b*) H. Sepehrmansourie, Silica sulfuric acid (SSA): As a multipurpose catalyst, *Iran. J. Catal.*, 2020, **10**, 175–179.

71 H. Sepehrmansouri, M. Zarei, M. A. Zolfigol, A. R. Moosavi-Zare, S. Rostamnia and S. Moradi, Multilinker phosphorous acid anchored En/MIL-100 (Cr) as a novel nanoporous catalyst for the synthesis of new *N*-heterocyclic pyrimido [4, 5-*b*] quinolines, *Mol. Catal.*, 2020, **481**, 110303.

72 H. Sepehrmansourie, M. Zarei, R. Taghavi and M. A. Zolfigol, Mesoporous ionically tagged cross-linked poly (vinyl imidazole) s as novel and reusable catalysts for the preparation of *N*-heterocycle spiropyrans, *ACS Omega*, 2019, **4**, 17379–17392.

73 E. Tavakoli, H. Sepehrmansourie, M. Zarei, M. A. Zolfigol, A. Khazaei and M. Hosseinifard, Applications of novel composite UiO-66-NH_2/Melamine with phosphorous acid tags as a porous and efficient catalyst for the preparation of novel spiro-oxindoles, *New J. Chem.*, 2022, **46**, 19054–19061.